

An improved description of charged Higgs boson production*

Johan Alwall

High Energy Physics, Uppsala Univ., Box 535, S-751 21 Uppsala, Sweden

E-mail: Johan.Alwall@ts1.uu.se

February 2, 2008

Abstract:

Many extensions of the Standard Model predict the existence of charged Higgs bosons. In order to be able to find those particles, an accurate description of their production is needed. In Monte Carlo simulations of charged Higgs boson production at hadron colliders, the two tree-level processes $gb \rightarrow H^\pm t$ and $gg \rightarrow H^\pm tb$ are used. Since those processes overlap in the collinear region of the phase-space of the outgoing b -quark, care must be taken not to introduce double-counting if both processes are to be used together. In this talk I present a method for matching these processes, developed by Johan Rathsman and myself. The method also allows for investigations of the factorization scale dependence of the processes and a better understanding of which factorization scale to choose to get a reliable description of charged Higgs production.

1 Introduction

The existence of a charged Higgs boson is a common feature of many extensions of the Standard Model of particle physics, most notably supersymmetric extensions such as the MSSM. In the Standard Model, the fermions get their mass from their interaction with the Higgs field, which gets a non-zero vacuum expectation value from spontaneous symmetry breaking of the isospin $SU(2)_L$ symmetry. The vector bosons W^\pm and Z^0 get mass by absorbing three of the originally four scalar degrees of freedom from the Higgs doublet. In supersymmetric extensions of the Standard Model, one Higgs doublet is not enough - at least two are necessary for mainly two reasons (see *e.g.* [1]):

1. The fermionic superpartner of the Higgs boson, so called higgsino, destroys the cancellation of the ABJ anomaly (see *e.g.* [2]) in the Standard Model. In order for the anomaly to cancel, two Higgs doublets (and thus two higgsinos) with opposite hypercharge are needed.

*Talk given at the 42nd International School of Subnuclear Physics at Erice, Sicily, 1 September 2004

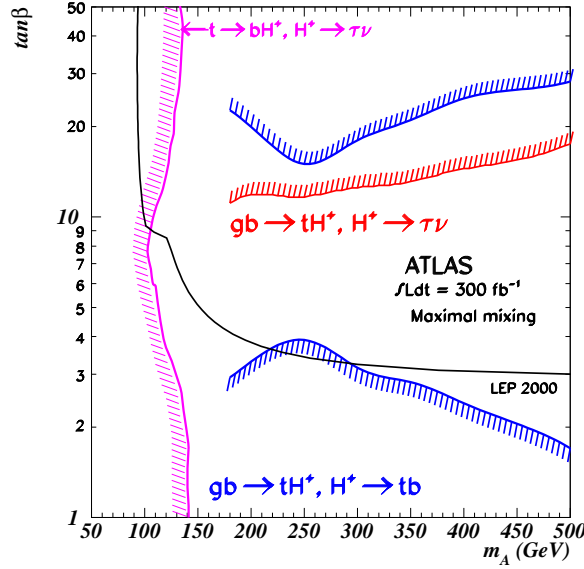


Figure 1: The ATLAS 5- σ discovery contour for charged Higgs. The gap in the region around the top mass could be bridged using a properly matched sum of the $gb \rightarrow H^\pm t$ process and the $gg \rightarrow H^\pm tb$ process. Figure taken from [3].

2. With supersymmetry, the same Higgs doublet cannot interact with (and hence give mass to) both the up-type (u, c, t) and the down-type fermions (d, s, b and the charged leptons).

With two Higgs doublets (8 real fields) but still only three massive vector fields, we get five surviving Higgs fields:

$$h, H, H^+, H^-, A \text{ (pseudoscalar)}$$

Such a theory is called a (type II) two Higgs doublet model (2HDM).

In the MSSM there are only two parameters determining the masses and interactions of these fields: the first is $\tan \beta = \frac{v_1}{v_2}$, the ratio of the vacuum expectation values for the two Higgs doublets, the second is one of the masses, *e.g.* the pseudoscalar mass M_A . In a general 2HDM, however, there are seven (or more) parameters.

Needless to say, the discovery of a charged scalar particle would be a clear signal of physics beyond the Standard Model. In order to search for such a particle, we need an accurate description of the production mechanisms and phase-space distributions. Using Monte Carlo programs, the production of charged Higgs can then be simulated, and one can optimize search strategies (*i.e.* minimize the Standard Model background) using different cuts on the data from the collider. Even before any actual experiment is done, one can in this way put limits on the parameter-space regions where different experiments will be able to find a signal (see fig. 1).

In Monte Carlo generators such as PYTHIA[4] and HERWIG[5], the production channels used to simulate single charged Higgs boson production (as opposed to pair-production,

which is not discussed here) are $g\bar{b} \rightarrow H^+\bar{t}$ and $gg \rightarrow H^+\bar{t}b$ and their charge conjugates. (There is also a process $q\bar{q} \rightarrow H^\pm tb$, which gives a large contribution in a $p\bar{p}$ -collider such as Tevatron, but a very small contribution at the high energies of the LHC.) Here (as usual) g stands for gluon and q (\bar{q}) for an arbitrary quark (antiquark). The $gg \rightarrow H^\pm tb$ process gives a better description of the part of phase-space where the outgoing b -quark has a large transverse momentum (p_T), while the $gb \rightarrow H^\pm t$ process resums potentially large logarithms $(\alpha_s \log(\mu_F/m_b))^n$ and hence give a better description in the rest of the phase space, as will be discussed later. In the region where the outgoing b -quark has small transverse momentum, the two processes overlap. Therefore, if both processes would be used and summed naively we would get double-counting in this region of phase-space. Together with Johan Rathsmann, I have developed a method to remove this double-counting by generating events from a distribution corresponding to the double-counted part of phase space, and subtracting these events from the sum. Our work is presented in [7], where also more references are found.

2 The twin-processes and their double-counting

As discussed in the introduction, the two tree-level processes (*i.e.* no-loop processes) used in Monte Carlo simulation of single production of charged Higgs at hadron colliders are

$$g\bar{b}(b) \rightarrow \bar{t}H^+ (tH^-) \quad (1)$$

$$gg \rightarrow \bar{t}bH^+ (t\bar{b}H^-) \quad (2)$$

The first one (1), which I will denote the leading order (LO) or $2 \rightarrow 2$ process, includes the b -quark density, $b(\mu_F^2) \sim \sum (\alpha_s \log(\mu_F/m_b))^n$, which comes from the logarithmic DGLAP resummation of gluon splitting to $b\bar{b}$ pairs. This means that the b -quark going into the process is accompanied by a \bar{b} (or vice versa) which is not explicitly shown in the equation. Due to the approximation made in the DGLAP expansion, this accompanying b -quark is nearly collinear with the beam. The second production process, (2), which I will denote the $2 \rightarrow 3$ process, gives the correct treatment of the kinematics of the accompanying b -quark to order α_s^2 . The relation between the two processes is illustrated in fig. 2. Since the processes really have the same initial and final states, they can be viewed as the same process in two different approximations, hence the term “twin-processes”.

As suggested by fig. 2, there is an overlap between the two processes: When the transverse momentum of the outgoing b -quark in the $2 \rightarrow 3$ process is small, there is no distinction between the full $2 \rightarrow 3$ matrix element and a gluon splitting to $b\bar{b}$ convoluted with the $gb \rightarrow H^\pm t$ matrix element. Therefore there is a double-counting between the processes, which can be expressed as [6]

$$\sigma_{\text{DC}} = \int dx_1 dx_2 \left[g(x_1, \mu_F) b'(x_2, \mu_F) \frac{d\hat{\sigma}_{2 \rightarrow 2}}{dx_1 dx_2}(x_1, x_2) + x_1 \leftrightarrow x_2 \right] \quad (3)$$

where

$$b'(x, \mu_F^2) = \frac{\alpha_s(\mu_R^2)}{2\pi} \int \frac{dQ^2}{Q^2 + m_b^2} \int \frac{dz}{z} P_{g \rightarrow q\bar{q}}(z) g\left(\frac{x}{z}, Q^2\right) \quad (4)$$

$$\approx \frac{\alpha_s(\mu_R^2)}{2\pi} \log \frac{\mu_F^2}{m_b^2} \int \frac{dz}{z} P_{g \rightarrow q\bar{q}}(z) g\left(\frac{x}{z}, \mu_F^2\right) \quad (5)$$

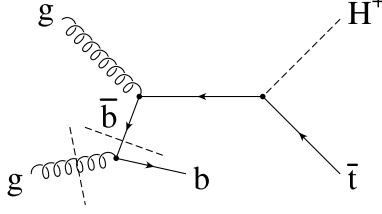


Figure 2: Illustration of the relation between the $gb \rightarrow H^\pm t$ and $gg \rightarrow H^\pm tb$ processes. If the factorization between the parton densities and the hard scattering is done at the gluon line we get the $gg \rightarrow H^\pm t\bar{b}$ process, while if instead this factorization is done at the \bar{b} line, we get the $g\bar{b} \rightarrow H^\pm \bar{t}$ process. They can therefore be viewed as the same process in two different approximations.

This is just the leading logarithmic contribution to the b -quark density included in the $2 \rightarrow 2$ process. Here $P_{g \rightarrow q\bar{q}}(z) = \frac{1}{2} [z^2 + (1-z)^2]$ is the splitting function for g going to $q\bar{q}$, μ_F is the factorization scale (*i.e.* the scale where the parton densities are evaluated) and μ_R is the renormalization scale used in evaluating α_s , and $Q^2 = -k^2$, the 4-momentum of the incoming b -quark squared. We need to take care to include kinematic constraints due to the non-zero b -quark mass in our calculation of the integration limits, since such constraints are implicitly included in the $2 \rightarrow 3$ matrix element. This is done in detail in our paper [7].

The matched integrated cross-section is then given by

$$\sigma = \sigma_{2 \rightarrow 2} + \sigma_{2 \rightarrow 3} - \sigma_{\text{DC}} \quad (6)$$

The matched integrated cross-section and its components are shown as a function of the charged Higgs boson mass in fig. 3. For charged Higgs masses below the top mass the cross-section can be well approximated by top pair production with subsequent decay of one of the top quarks to $H^\pm b$, *i.e.* $gg \rightarrow t\bar{t} \rightarrow tbH^\pm$ (for a comparison between this process and the $2 \rightarrow 3$ process, see [8]). Our matching procedure works for all charged Higgs masses, but is of greatest interest for $m_{H^\pm} \gtrsim m_t$. In the following I will use $m_{H^\pm} = 250$ GeV and $\tan \beta = 30$ as a case study.

3 Matching the differential cross-sections

As we saw in the last section, the cancellation of the double-counting between the $2 \rightarrow 2$ and $2 \rightarrow 3$ processes on the integrated cross-section level was simple enough. But how do we do it for the differential cross-sections? Whatever approach we take, we need to make sure some basic requirements are fulfilled:

1. The integrated cross-section should equal the correct one given by eq. (6).
2. All differential cross-sections should be smooth after matching.
3. The matched p_T -distribution for the outgoing b -quark should be given by the $2 \rightarrow 2$ process for small transverse momenta, and by the $2 \rightarrow 3$ process for large transverse momenta, with a smooth interpolation between those regions.

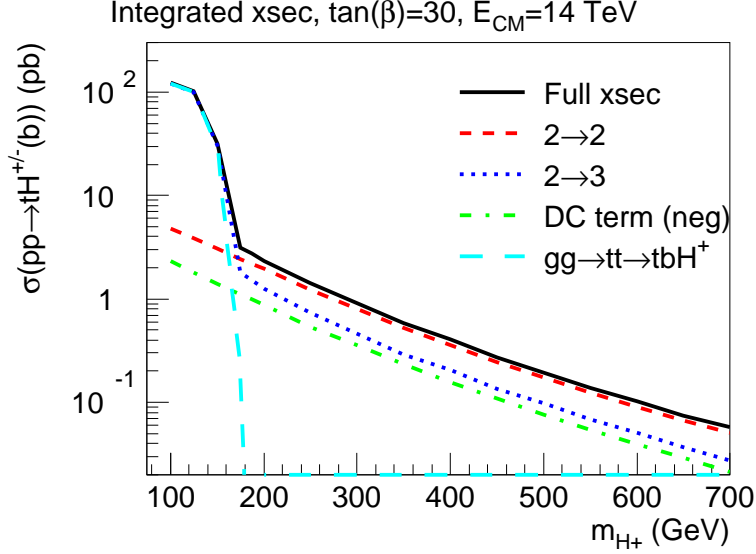


Figure 3: Integrated cross-section components (leading order process, $2 \rightarrow 3$ process and double-counting term) and matched total as a function of the H^\pm mass at LHC, with $\tan\beta = 30$ and $\mu_F = (m_t + m_{H^\pm})/4$. Note that the double-counting term contribution (DC) is subtracted from the sum. At $m_{H^\pm} < m_t$ the $2 \rightarrow 3$ process can be approximated by $gg \rightarrow t\bar{t} \rightarrow tbH^\pm$.

A Monte Carlo event generator simulates collision events by picking kinematical variables from a probability distribution given by the folding of parton density functions with the matrix element of the hard scattering. In this way the events will be distributed in all kinematic variables according to the differential cross-section distribution of the process in question. This is true for the $2 \rightarrow 2$ process as well as for the $2 \rightarrow 3$ process. The number of events generated for each process is proportional to the integrated cross-section of the process. In a process where we have an incoming b (\bar{b}), such as the $2 \rightarrow 2$ process, we get an accompanying outgoing \bar{b} (b) from the gluon splitting as explained above. The kinematic distribution of this accompanying \bar{b} is given by the DGLAP evolution and generated through so called parton showers (PS) (see *e.g.* [4]).

Now, our solution to the matching problem is simple: We view the double-counting term (given by eq. (3)) as a probability distribution in kinematic variables and pick events from this distribution. Then we subtract this contribution (*i.e.* add with negative weight) from the sum of the two processes (1) and (2) in the final data analysis, *i.e.* the histograms.¹

One might worry that this procedure could give a negative number of events in some phase-space region. However, the leading-logarithmic part of the b density used in the double-counting term is always smaller than the full b density used in the $2 \rightarrow 2$ process, ensuring that if only a sufficiently large number of events is generated, the sum of the events from the $2 \rightarrow 2$ and the $2 \rightarrow 3$ process will always be larger than the number of events from the

¹The code for the double-counting term, implemented as an external process to PYTHIA, will be available for download at <http://www3.ts1.uu.se/thep/MC/pytbh>, including a manual in preparation.

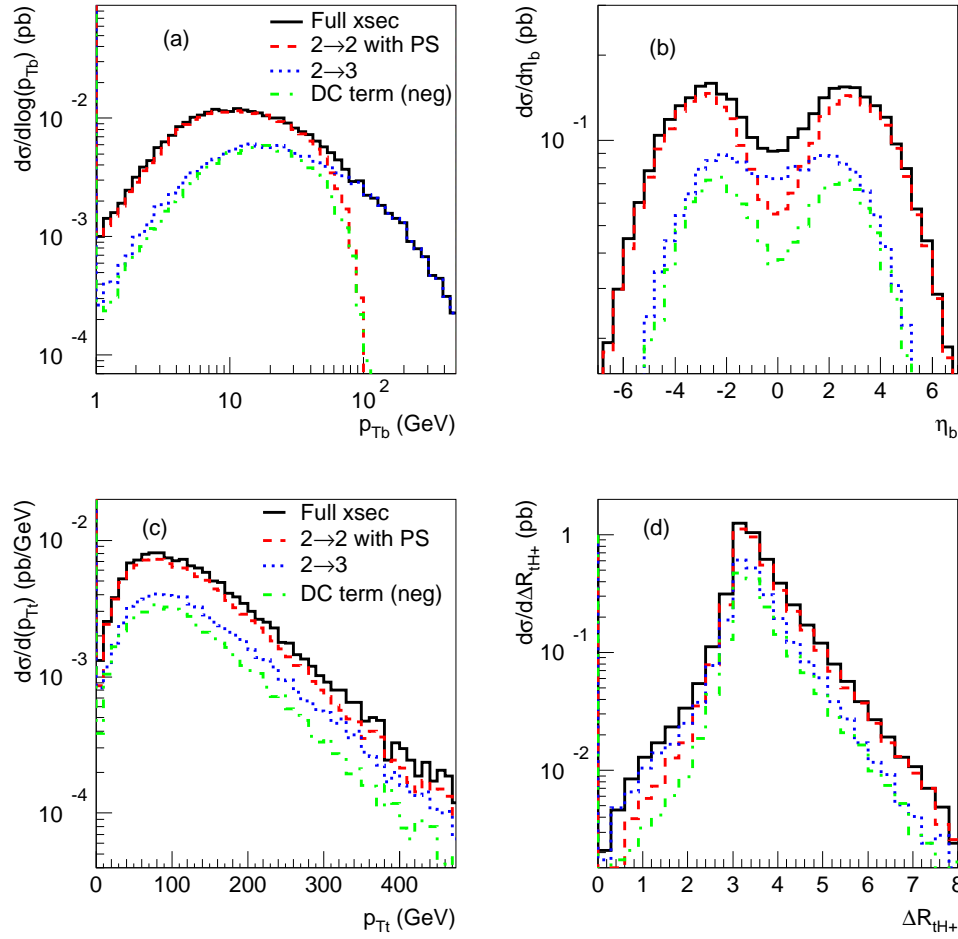


Figure 4: Differential cross-sections in (a) $p_{T,b}$, (b) η_b , (c) $p_{T,t}$ and (d) $\Delta R_{H^\pm t}$ for the cross-section components and the resulting matched cross-section with $\tan \beta = 30$, $m_{H^\pm} = 250$ GeV and $\mu_F = (m_t + m_{H^\pm})/4$. Note that the double-counting term contribution (DC) is subtracted from the sum.

double-counting term.

Some resulting differential cross-sections from our matching are shown in fig. 4. Looking at fig. 4a we see that the matched differential cross-section in p_T for the outgoing b -quark looks exactly as expected (and wanted): for small p_T it follows the $2 \rightarrow 2$ process distribution, while for large p_T it follows the $2 \rightarrow 3$ process. However, there is a rather large intermediate region, from about 30 GeV to about 100 GeV, where the whole matching procedure is really necessary to get the correct differential cross-section. For comparison one can note that at LHC, the region where b -quarks can be tagged is $p_{T,b} \gtrsim 20$ GeV. In fig. 4b we see large differences in the rapidity distribution for the outgoing b -quark between the matched cross section and each of the two contributing processes, up to a factor $\simeq 2$ in the experimentally interesting region $|\eta_b| < 2.5$, indicating that matching is really necessary to get a correct description of the b -quark kinematics..

Even if the outgoing b is not observed, we still see a difference between the matched cross-section and the $2 \rightarrow 2$ process, which is usually used in this case. In the transverse momentum distribution of the top quark (fig. 4c) we get a small enhancement for large $p_{T,t}$, amounting to $\sim 20\%$ compared to the $2 \rightarrow 2$ process. There is a similar effect in the distribution of the charged Higgs boson (not shown). In fig. 4d, showing the distance measure $\Delta R_{H^\pm t} = \sqrt{\Delta\varphi_{H^\pm t}^2 + \Delta\eta_{H^\pm t}^2}$, we see an effect especially for small separations.

All in all, we see that unless we make very limiting cuts on the phase space, we need to use the matched differential cross-sections to get reliable predictions.

4 Factorization scale dependence

The factorization scale is the scale where the factorization is done between the parton description of the proton and the hard scattering of the partons, *i.e.* where the parton distributions are evaluated. This scale also determines the maximum transverse momentum of the parton shower, *e.g.* of the outgoing b -quark of the $2 \rightarrow 2$ process. Of course, the factorization scale, just like the renormalization scale, is a fictitious entity in the sense that if all orders of perturbation theory was included in the cross-section calculation, the scale would never show up in the result. However, in real life we can only use a few orders in perturbation theory, and then it is necessary to introduce such scales. Often the factorization scale is chosen to be some hard scale of the process, *e.g.* the invariant mass \hat{s} of the partonic system or the transverse mass of one of the outgoing particles. In the process we are discussing, $gb \rightarrow H^\pm t$, often $m_{H^\pm} + m_t \approx \hat{s}$ is used as the factorization scale. What scale we should use in the lower-order calculations can not really be known until all orders of perturbation theory have been calculated, but the factorization scale dependence should be weaker the more orders we include. Therefore we get an indication of which scale to use in the first-order expression already by doing the next-to-leading order calculation.

The double-counting term of eq. (3) is designed to describe the part of the $2 \rightarrow 3$ process which is already included in the $2 \rightarrow 2$ process through the resummation of logarithmic contributions to the b -quark density. This means that the double-counting term should not exceed the $2 \rightarrow 3$ process contribution in any part of the phase-space. However, the upper integration limit of the transverse momentum of the outgoing b -quark in the double-counting term is determined by the factorization scale. Up to this limit the transverse momentum-distribution is almost flat, which means that the integrated value of the double-counting term is nearly proportional to the factorization scale (although for large scales the kinematic constraints modify this behaviour). This is illustrated in figs. 5 and 6.

Fig. 5 shows the integrated cross-section components, as well as the matched total, as a function of the factorization scale μ_F parametrized by $\rho = \mu_F/\overline{m}$, where $\overline{m} = (m_{H^\pm} + m_t)/2$ is the average of the charged Higgs and top masses. Here two things can be noted. The first is that the double-counting term exceeds the $2 \rightarrow 3$ process term already near $\rho = 1$, *i.e.* $\mu_F \gtrsim (m_{H^\pm} + m_t)/2$. This indicates that the factorization scale should definitely not be chosen above this value. The other thing to be noted is that the matched integrated cross-section shows a significantly smaller dependence on the factorization scale than any one of the component cross-sections, indicating that the matching also stabilizes the cross-section. This is not surprising, since the $2 \rightarrow 3$ process is a part of the next-to-leading order calculation of

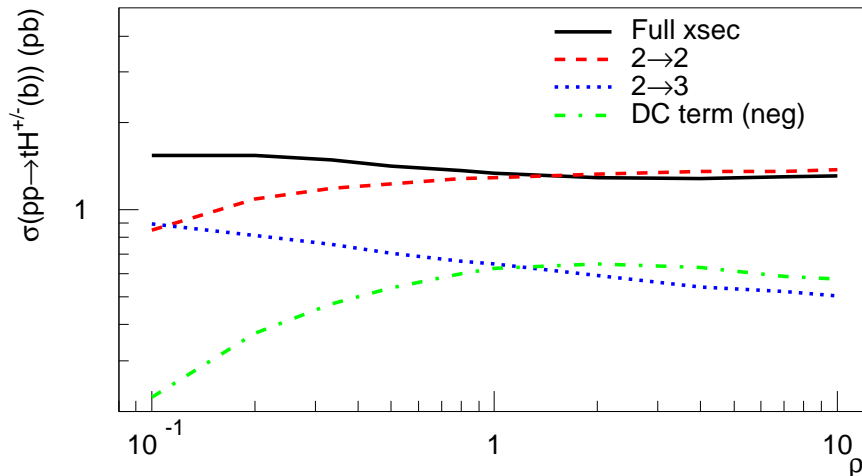


Figure 5: Integrated cross-sections at $m_{H^\pm} = 250$ GeV and $\tan\beta = 30$ as a function of the factorization scale parametrized by $\rho = 2\mu_F/(m_t + m_{H^\pm})$. Note that for $\rho \gtrsim 1$ the double-counting term exceeds the $2 \rightarrow 3$ term. Also note that the factorization scale dependence is smaller for the matched total cross-section than for any one of the components.

the $2 \rightarrow 2$ process. Hence including it in a correct way should reduce the factorization scale dependence, as is the case when calculating the full next-to-leading order expression.

In fig. 6 we see the distribution in p_T of the outgoing b -quark for the $2 \rightarrow 3$ process (without parton showers) and the double-counting term at different factorization scales. Here we see that already for $\rho = 1$, the double-counting term exceeds the $2 \rightarrow 3$ term around $p_{T,b} \approx 50$ GeV. $\rho = 0.5$, *i.e.* $\mu_F = (m_{H^\pm} + m_t)/4$, seems to be a limiting case where the double-counting distribution just touches the $2 \rightarrow 3$ -distribution. Therefore we have chosen to use this unconventionally small value of the factorization scale in our plots in the previous sections. Similar results for the size of the factorization scale has been achieved in next-to-leading order calculations of the $2 \rightarrow 2$ process, see [9, 10].

5 Conclusions

The discovery of a charged scalar particle would be a clear signal of physics beyond the Standard Model of particle physics. The detailed study of the properties of such a particle would give valuable insight into the nature of this new physics. But to be able to find the charged Higgs boson, we need to devise search strategies and to reduce the Standard Model background. For this, an appropriate description of charged Higgs boson production, using Monte Carlo events generators, is necessary.

For single charged Higgs boson production, mainly two processes are used in Monte Carlos, the bottom-gluon fusion $gb \rightarrow H^\pm t$ production channel and the gluon-gluon fusion $gg \rightarrow H^\pm tb$ channel. These have different virtues: $gb \rightarrow H^\pm t$ resums large logarithms describing the b -quark density, why it gives the major contribution to the total cross-section,

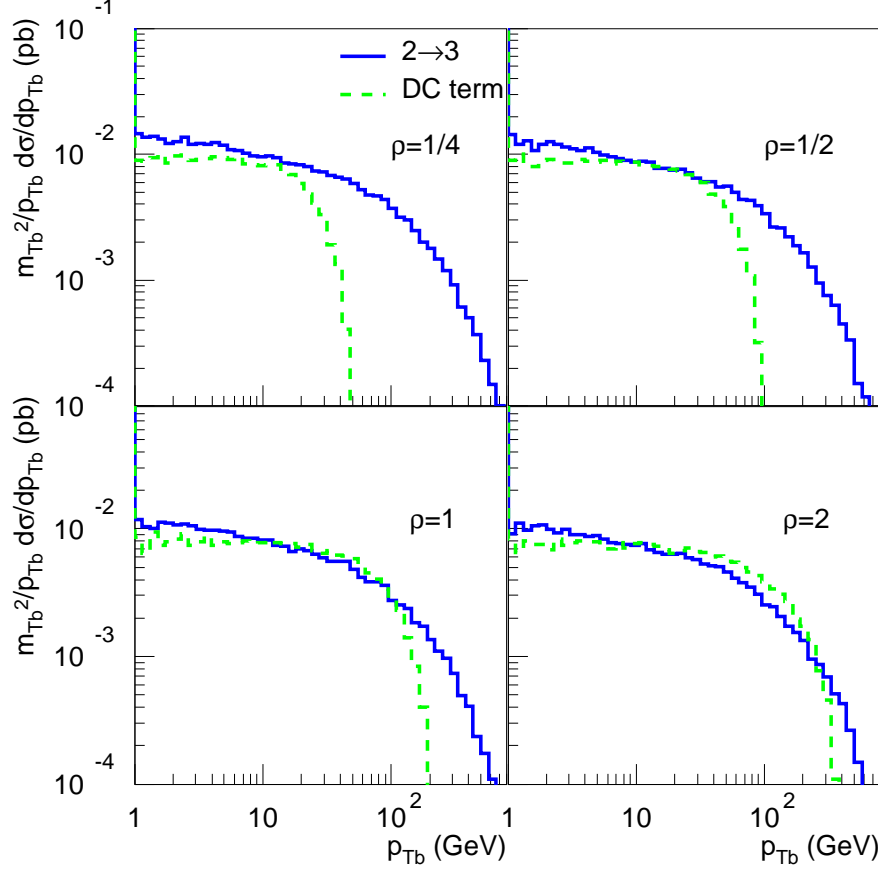


Figure 6: The differential cross-section $d\sigma/dp_{T,b}$ multiplied by $m_{T,b}^2/p_{T,b}$ for the $2 \rightarrow 3$ matrix element and the double-counting term for different factorization scales parameterized by $\rho = 2\mu_F/(m_t + m_{H^\pm})$. Note that the double-counting term overshoots the $2 \rightarrow 3$ term already for $\rho = 1$.

and also gives the best description of the differential cross-section for small values of the transverse momentum of the associated b -quark. On the other hand, the $gg \rightarrow H^\pm tb$ process gives a correct description to order α_s^2 of the outgoing b -quark for large values of the transverse momentum. However, the two processes overlap in the small transverse momentum region, so in order to use them both we must compensate for this double-counting.

In this talk I have presented our algorithm for the matching of the two processes. This matching is done by summing the events from the two processes (as is usually done in Monte Carlo generators), and then subtract events generated from a double-counting distribution term from the sum. In this way we are able to combine the virtues of the two processes to get a good description of the full differential cross-section.

This method also allows us to get a better understanding of what choice of factorization scale is appropriate, by comparing the transverse momentum distributions for the double-counting term with the distribution for the $2 \rightarrow 3$ process matrix element. Since the double-counting term should remove the part of the $2 \rightarrow 3$ distribution already contained in the

$2 \rightarrow 2$ distribution, the double-counting term should not overshoot the $2 \rightarrow 3$ term. The result is that the appropriate factorization scale is significantly smaller than the conventionally used value.

Acknowledgements:

I would like to thank the organizers of ISSP42 for giving me the opportunity to present this talk. I would also like to thank all participants of the school for giving me a great time.

References

- [1] S. Dawson, “SUSY and such,” arXiv:hep-ph/9612229.
- [2] T. P. Cheng and L. F. Li, *Gauge Theory Of Elementary Particle Physics*, Oxford science publications, 1984
- [3] K. A. Assamagan and Y. Coadou, Acta Phys. Polon. B **33** (2002) 1347.
- [4] T. Sjöstrand *et al.*, “High-energy-physics event generation with PYTHIA 6.1,” Comput. Phys. Commun. **135** (2001) 238 [arXiv:hep-ph/0010017].
- [5] G. Corcella *et al.*, “HERWIG 6: An event generator for hadron emission reactions with interfering gluons (including supersymmetric processes),” JHEP **0101** (2001) 010, [arXiv:hep-ph/0011363].
- [6] F. Borzumati, J. L. Kneur and N. Polonsky, “Higgs-strahlung and R-parity violating slepton-strahlung at hadron colliders,” Phys. Rev. D **60** (1999) 115011 [arXiv:hep-ph/9905443].
- [7] J. Alwall and J. Rathsman, “Improved description of charged Higgs boson production at hadron colliders,” arXiv:hep-ph/0409094.
- [8] J. Alwall, C. Biscarat, S. Moretti, J. Rathsman and A. Sopczak, “The p anti- $p \rightarrow t$ b H^{\pm} process at the Tevatron in HERWIG and PYTHIA simulations,” in *The Higgs working group: Summary report 2003*, arXiv:hep-ph/0312301.
- [9] T. Plehn, “Charged Higgs boson production in bottom gluon fusion,” Phys. Rev. D **67** (2003) 014018 [arXiv:hep-ph/0206121].
- [10] E. L. Berger, T. Han, J. Jiang and T. Plehn, “Associated production of a top quark and a charged Higgs boson,” arXiv:hep-ph/0312286.